Face Recognition Attendance System Method Based on Fusion of LBP and HOG

Vrunda Mahajan[1] and Dr. Priti Subramanium[2]
Student, Department of Computer Science and Engineering [1]
Assistant Professor, Department of Computer Science and Engineering[2]
Shri Sant Gadge Baba College of Engineering and Technology, Bhusawal, Maharashtra, India

Abstract: *As one of the hot topics in the field of computer vision research, face recognition technology has received significant attention due to its potentiality for a wide range of applications in government as well as commercial purposes. In practical applications, although several existing face recognition methods have achieved good performances in specific scenes, they easily suffer from a sharp decline in recognition rate if affected by different conditions of light, expression, posture and occlusion. Among many factors, influences of complex illuminations on face recognition are particularly significant. To further improve the performance of the existing local binary pattern (LBP) operator, neighbourhood weighted average LBP (NWALBP) is first proposed for fully considering the strong correlations between pixel pairs in the neighbourhood, which extends the traditional LBP uni-layer neighbourhood template window to the bi-layer neighbourhood template window and calculates the weighted average of bi-layer neighbourhood pixels in each direction. Then, inspired by centre symmetric LBP (CS-LBP), centre symmetric NWALBP (CS-NWALBP) is further proposed, which can effectively reduce computation complexity by only comparing the weighted average values of the neighbourhood pixels that are symmetric about the centre pixel. Finally, by combining the merit of histogram of oriented gradient (HOG), a feature fusion algorithm named CS-NWALBP+HOG is suggested. Several experiments have eventually demonstrated that our proposed algorithms have more robust performance under complex illumination conditions if compared with many other latest algorithms.*

Keywords: Face recognition, Histograms of gradients, Local binary pattern.

I. INTRODUCTION

As one of the hot topics in the field of computer vision research, face recognition technology has received significant attention due to its potentiality for a wide range of applications in government as well as commercial purposes, such as law enforcement, counter terrorism, border control, e-commerce, voter identification, banking etc. Through the efforts of several research and commercial institutions, many achievements have been made and face identification system can work very well under certain ideal acquisition conditions. However, its performance will be inevitably affected by many factors [1, 2], including lighting conditions, facial expressions, occlusions, clutters, pose variations, aging, background, skin colour etc. In fact, if capturing the object images under good lighting conditions, it is relatively easy to obtain great identification performance. But the recognition results may become very poor if the object images are captured under uneven illumination, insufficient illumination, excessive illumination etc. The reason is that the difference between images from the same face sometimes is likely to be greater than the difference between images from different faces [3, 4]. Therefore, researchers put forward a series of improved solutions to overcome the above-mentioned problem, which can be divided into three categories, including image prepossessing algorithms, feature extraction algorithms based on spatial transformations, as well as feature extraction algorithms based on local features. The idea of image pre-processing algorithms is adopting various types of image enhancement methods before face recognition. There are four kinds of commonly used enhancement methods [5, 6]: grey level transformation with histogram equalisation as the representative [7, 12], homomorphic filtering base on illumination reflectance model [13, 18], light compensation based on Retinex theory [19, 24], as well as image enhancement in gradient domain [25, 30]. Grey level transformation based on global histogram equalisation can enhance image's overall contrast and is suitable for enhancing images which have lower overall grey value or dynamic range. Grey level transformation based on local

histogram equalisation can enhance image's detail information and expand local greyscale range, but may lead to the block effect and lower calculation rate etc. Both homomorphic filtering and Retinex light compensation are frequency domain processing methods, and their computational efficiency are relatively high. Homomorphic filtering can be used to enhance images which have low local grey level value and high dynamic range, but it may cause over-enhancement phenomenon and suffer from poor performance in the highlight and shadow regions. Retinex theory is mainly used to estimate image brightness and compensate detail information in dark regions while maintaining the brightness of the whole image. However, Retinex light compensation inevitably adjusts some parameters for each image, and its processing capability in the brighter region is very poor. Light halos are easy to appear in the regions where there are large variations of the gradient values. Gradient domain enhancement can expand local gradient range while compressing overall dynamic range. Compared with other methods, it performs well in enhancing image shadow and highlight regions, but needs to reconstruct the image in gradient domain by certain numerical algorithms. In recent years, the above four kinds of methods are constantly improving. Histogram equalisation methods tend to combine with human vision, enhancing the image while preserving its original appearance. Homomorphic filtering and Retinex light compensation methods tend to combine with other methods, and their function of reducing noise can make up for the shortcomings of other methods. The gradient domain methods focus on the improvement of computational efficiency. However, there are still two main drawbacks for these image enhancement methods: (1) computational efficiency: although local histogram equalisation or gradient domain method work very well, their practical applications are limited by lacking fast computing algorithms, and are more suitable for image analysis without any real-time requirement; (2) application scope: all these image enhancement methods are based on the assumption that the greyscale value variations of the image are continuous and slow. However, when light reflections appear in certain regions, the grey level value variations of the image are great, and the histogram equalisation method become invalid because of this large dynamic range. If the grey level variations for one part of the image are continuous and slow, but for the other part are burst, the homomorphic filtering and Retinex light compensation methods will also fail to work. Although the gradient domain method can extract the burst location of the image, it is still difficult to avoid the influence of severe illumination variations on the image.

As the second kind of the face recognition methods, feature extraction algorithms based on spatial transformations can transform image information of high-dimensional subspaces into image information of low-dimensional subspaces with more discriminating abilities, by utilising mathematical transformation theory to realise feature extraction. Two typical feature extraction algorithms are respectively principal component analysis (PCA) [31] and singular value decomposition (SVD) [32]. They first calculate the covariance matrix of the data set, then select a certain number of orthogonal bases to construct a projection subspace, which has relatively lower dimensions than that of original data set, and in the meanwhile can preserve the original information after subspace reconstruction to the maximum extent. 'Eigenface' can be obtained after dimension reduction, but it represents the global information of the face image and does not consider the local information, thus leads to lower recognition rate. Many improved algorithms based on PCA or SVD are proposed, such as kernel PCA (KPCA) [33], modular PCA (MPCA) [34], two dimensional PCA (2DPCA) [35, 36], weighted subpattern PCA (Aw-SpPCA) [37], discriminative K-SVD (DK-SVD) [38], flustered SVD (FSVD) [39], but their performances are still not very good especially under complex illumination. Therefore, a series of improved algorithms are further proposed by combining with other methods, such as wavelet transform [40, 41], correlation filter [42], linear discriminant analysis (LDA) [43], retina modelling [44], virtual representation [45] etc. Moreover, in order to utilise samples' high-order statistical characteristics, other algorithms are proposed, such as linear discriminant analysis (IDA) [46], discrete cosine transform (DCT) [47] etc. However, all algorithms mentioned above can only work well under the premises of sufficient available training samples and expensive calculating costs, which are indeed some inevitable obstacles for practical applications. More importantly, all of them are global feature extraction methods and can only obtain an image's overall information, thus they are very sensitive to local light and noise, and their capabilities to describe image's local texture details are barely satisfactory, especially under complex illumination variations nation variations.

The main idea of the third kind of algorithm based on local feature extraction is as follows: dividing the whole image into several blocks and extracting key features for each block; then concatenating these corresponding features according to certain rules; finally, obtaining the eventual feature descriptions for the whole original image. Compared

with the above-mentioned global feature extraction algorithms, local feature extraction algorithms always have stronger description abilities to image texture details and perform better robustness to illumination, noise, pose variations etc. Furthermore, among all the local feature extraction algorithms, local binary pattern (LBP) [48], histogram of oriented gradient (HOG) [49] and Weber local descriptor (WLD) [50] are the classical representative local descriptors since they can explore local illumination insensitive characteristics very well. The original LBP operator [48] is used to describe local image texture features by comparing the grey value of central pixel with each that of its eight surrounding neighbour pixels and calculating the image contrast within the templet of pixels 3*3. LBP operator is easy to be carried out and efficient, and it has the advantages of rotational invariance, as well as greyscale invariance, but it is difficult to meet various requirements of roughness and texture sizes for image identification in the practical applications. An improved circular LBP operator [51] is proposed by expanding the templet from pixels 3*3 with radius 1 to circular area with any radius value. However, it will lead to a significant increase in computation complexity. To solve the above problem, a further improved method called center symmetric LBP (CS-LBP) [51] is given and received extensive attention, which can significantly reduce the computational dimensions. Over the next years, many experts and scholars have proposed a variety of improved algorithms based on LBP, including Bayesian LBP (BLBP) [53], complete LBP (CLBP) [54], weighted LBP with adaptive threshold (W-LBPAT) [55], Multi-scale block LBP (MB-LBP) [56] etc, and all of them further enhance the description ability for texture details. HOG [57] is a kind of commonly used feature descriptor for computer vision, which can utilise local gradient histogram to describe local image region's edge and direction information very well. In view of the fact that HOG has strong robustness to light intensity and direction, several extended algorithms are given based on it. Some approaches based on HOG multi-feature fusion are proposed [58, 59], and the dimensions of holistic and local HOG features are reduced by using PCA or 2DPCA and LDA, which not only significantly raise the recognition rate and reduce the computing time but also has certain robustness to the influence of light. A method called layered fusion of CS-LBP and HOG feature is proposed to better capture image's edge information and thus improve recognition rate greatly [60]. Inspired by Weber's law, a simple yet very powerful and robust local descriptor called WLD is proposed based on the fact that human perception of a pattern depends not only on the change of a stimulus (such as sound, lighting) but also on the original intensity of the stimulus [50]. WLD consists of two components: differential excitation and orientation, and these two components construct a concatenated WLD histogram. It is revealed that WLD only utilises the texture information of the central pixel's surrounding pixels from the nearest neighbourhood layer, but the central pixel's excitation is also related to the texture information of its surrounding pixels from the outer neighbourhood layer, thus some key local texture information is not utilised sufficiently, leading to performance loss [61]. To solve the above problem, many optimal algorithms are suggested based on WLD. A local descriptor called Weber local binary pattern (WLBP) is proposed by effectively combining the advantages of WLD and LBP [62]. WLBP is a powerful texture descriptor including two components: differential excitation and LBP. The differential excitation extracts perception features by Weber's law, while LBP can describe local features splendidly. A method for face recognition using multi-scale WLDs and multi-level information fusion is presented [63]. Based on the local graph stucture (LGS) [64] and its improved symmetric-local LGS (SLGS) [65], a novel image feature representation descriptor called orthogonal symmetric local Weber graph structure (OSLWGS) is presented to further enhance recognition capability by fusing the merits of WLD and LGS [66]. There are also many other improved algorithms which can obtain stronger robustness to complex illumination and noise, such as local difference ternary sequences (LDT) [67], Weber synergistic center-surround pattern (WSCP) [68], local partial differential equation (L-PDE) [72] etc. Based on the classic deep learning net, many improved algorithms have been proposed. Some representative methods include VGGNet [73], ResNet [74], CNN+LBP [75], Spatial FCN [76], Crowd understanding [77, 78] and more, which easily suffer from the insufficient training sample.

In practical applications, although the existing face recognition algorithms have achieved good results in specific scenes, they are easily affected by illumination, expression, posture and occlusion, leading to a sharp decline in recognition rate. Among many influencing factors, complex illumination has a particularly significant impact on face recognition. To obtain a good image description method which is insensitive to illumination, this paper proposes an improved fusion local feature extraction algorithm called CS-NWALBP+HOG. One important contribution of this paper is our proposed novel operator called CS-NWALBP, which not only smooths noise sensitivity of LBP operator but also reduces the original computational complexity, as well as strengthens the description ability for image gradient

direction information. There are four steps in the implementation of CS-NWALBP: extending the original uni-layer neighbourhood model of LBP to an improved bi-layer neighbourhood model; then calculating the weighted average values of pixels from each direction in the bi-layer neighbourhood; next, comparing the weighted average values of pixels that are symmetrical near the central pixel; last, coding a series of comparing results according to certain rules. Moreover, a novel fusion algorithm is proposed by combining the merits of HOG and CS-NWALBP for further promoting a robust performance under illumination variations. Several experiments are conducted to verify the effectiveness of our proposed algorithm CS-NWALBP+HOG, and it has better performance compared with many other existing methods.

The contributions of this paper are summarised as:

- To improve the effectiveness of the local binary pattern (LBP) operator, neighbourhood weighted average LBP (NWALBP) is first proposed by fully considering the strong correlations between pixel pairs in the neighbourhood.
- We propose one novel operator called CS-NWALBP, which not only smooths noise sensitivity of LBP operator but also reduces the original computational complexity.
- By utilising with the advantages of CS-NWALBP and HOG, a feature fusion algorithm named CS-NWALBP+HOG is suggested.

This paper is organized as follows: Section I provides an overview of the background of face recognition, and gives comprehensive evaluations of the latest mainstream methods as well as our contributions. Section II introduces the original LBP and HOG. Section III describes our proposed NWALBP and CSNWALBP in great detail, as well as presents a novel fusion algorithm based on HOG and CS-NWALBP to further overcome illumination sensitivities. Several experiments based on typical public databases are conducted and their corresponding performance comparisons are presented in Section IV. Section V provides a conclusion and suggests the future research works.

x_0	x_1	x_2
x_7	x_c	x_3
x_6	x_8	x_4

Fig. 1. The original LBP template window with a size of 3 * 3.

II. RELATED WORKS

2.1 LBP

LBP proposed by Ojala et al. [48] as early as 1996 has been widely used for face recognition and showed its high discriminative power for texture classification under complex illumination. LBP is a non-parametric operator which is described as an ordered set of binary comparisons of pixel intensities between the centre pixel and its eight surrounding pixels. Figure 1 shows the original LBP template window with a size of 3*3, and the LBP code can be expressed as Equations (1) and (2):

$$LBP_{P,R} = \sum_{i=0}^{P-1} s(x_i - x_c)2^i \qquad (1)$$

$$s(x) = \begin{cases} 1, & if\ x \geq 0 \\ 0, & if\ x < 0 \end{cases} \qquad (2)$$

Where x_c corresponds to the grey value of a center pixel, x_i to the grey value of the eight surrounding pixels. P represents the total number of the centre pixel's surrounding pixels and is equal to 8 for the original LBP operator. R is the radius of LPB template which is shown in Figure 1 and is equal to 1 for the original LBP operator. The calculation procedure of one LBP code example is illustrated in Figure 2. For any pixel, the original LBP operator only accounts for its relative relationship with its neighbour pixels, which makes itself insensitive to illumination intensities.

The original LBP operator extracts local features by utilising a template window with a size of 3*3, and it may confront with the problem that the range is too small to meet the needs of texture feature extraction with different sizes. Therefore, Ojala et al. extended the original LBP operator to circular LBP operator that can be with different sizes, and its calculation procedure is the same as that of the original LBP operator [51]. Several circular LBP operators with different values of P and R are shown in Figure 3.

The original LBP and its extended circular ones mainly compare local centre pixel's grey value with each grey value of its surrounding pixels and represent image's local features by their relative variations. Because of its simple calculation process, strong local description ability for texture details and good robustness to complex illuminations, LBP is widely used in image recognition and many other fields. However, if evaluating the effect of the original LBP and its extended circular ones, the grey values between the centre pixel and all of its surrounding neighbour pixels should be compared, and then rather long histograms may be produced but difficult to use in the context of a region. If the number of training sets is too large, it will further lead to the problem of slow system calculating operation and long feature extraction time. To address the problem, an improved LBP called CS-LBP was proposed which modified the scheme of comparing the pixels in the neighbourhood instead of comparing each pixel with the centre pixel [52]. The CS-LBP code can be expressed in Equations (3) and (4), and Centre symmetric pairs of pixels are compared as illustrated in Figure 4.

$$CS - LBP \sum_{i=0}^{P/2-1} s(x_i - x_{i+P/2})2^i, P = 8 \qquad (3)$$

$$s(x) = \begin{cases} 1, & if \ x \geq 0 \\ 0, & if \ x < 0 \end{cases} \qquad (4)$$

It can be seen in Figure 4 that for eight neighbours, LBP produces 256 different binary patterns, whereas for CS-LBP this number is only 16. Therefore, CS-LBP can effectively reduce the number of comparisons, and improve computational efficiency. Figure 5 shows example image 'LENA' and its corresponding feature images extracted respectively by LBP and CS-LBP.

2.2 HOG

Histogram of oriented gradient (HOG) was initially described by Dalal et al. in the context of person detection [49], and now widely used in pedestrian detection and face recognition. In HOG, gradient histograms are used to extract local features, which can well describe the edge and direction information, and thus have strong robustness to lighting, direction as well as other factors.
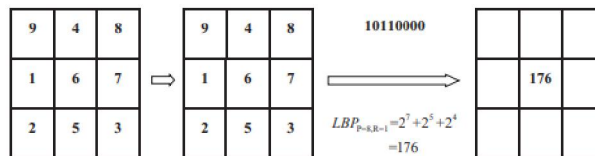

Fig. 2. The calculation procedure of one original LBP code example.
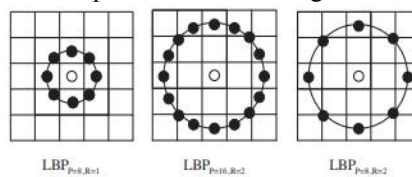

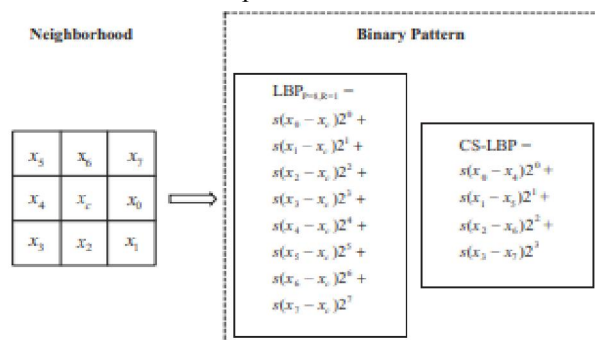Fig. 3. Several circular LBP operators with different values of P and R.

Fig. 4. Different comparing schemes of LBP and CS-LBP in the template window with a size of 3*3.

The implementation procedure of HOG is as follows: using a sliding window with fixed size to divide the target image into several blocks with certain overlaps; further dividing each block into small cells; then calculating the gradient

direction and amplitude of the grey value for each pixel; and calculating the corresponding histogram for each cell; finally, concatenating these cell histograms from each block to form the final statistical histogram as the feature extraction image.

Taking the target image with a size of 120*120 that is affected by illuminating variations as the example, feature extraction procedure of HOG is given as follows: first, carrying out greyscale transformation for the input target image, so as to reduce the interference from colour information when calculating the corresponding gradient values; second, utilising the sliding window with a size of 20*20 to obtain blocks; third, dividing each block into four cells uniformly and calculating the horizontal gradient Gh as well as vertical gradient Gv of pixel I(x,y) to obtain the marginal information, as given in Equations (5) and (6), thus, responding gradient values; second, utilising the sliding window with a size of 20*20 to obtain blocks; third, dividing each block into four cells uniformly and calculating the horizontal gradient G_h as well as vertical gradient G_v of pixel I(x,y) to obtain the marginal information, as given in Equations (5) and (6), thus,the corresponding gradient direction d (x,y) and the amplitude a(x,y) can be calculated as shown in Figures 7 and 8, respectively; fourth, dividing the range of [0, 180◦] uniformly into 20 regions with nine gradient directions, and making statistics on features according to which region that each pixel from each cell belongs to; fifth, obtaining the block statistical histogram by concatenating each statistical histogram of cells and standardizing the extracted features to relieve the influence of illumination variation, noise as well as other factors; finally, obtaining the entire statistical histogram features for the target image by concatenating each standardized histogram of blocks:

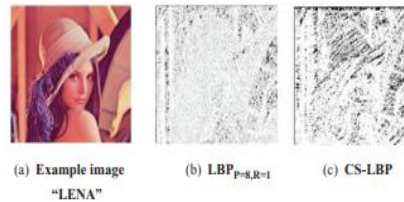(a) **Example image** "LENA" (b) **LBP**$_{P=8,R=1}$ (c) **CS-LBP**

Fig. 5. Example image 'LENA' and its corresponding feature images.
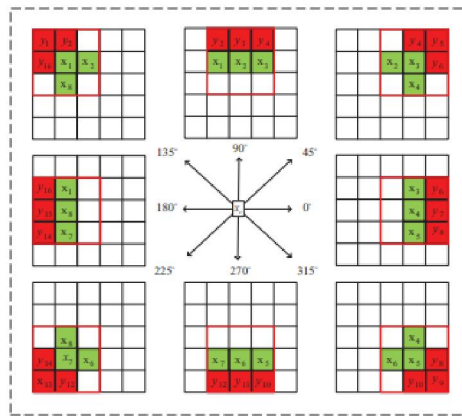

Fig. 6. The inner and outer layer neighbourhood pixels in different directions of NALBP template window.

$$\begin{bmatrix}0 & 2 & 1\\0 & 2 & 1\\0 & 2 & 1\end{bmatrix}\begin{bmatrix}0 & 1 & 1\\2 & 2 & 1\\0 & 2 & 0\end{bmatrix}\begin{bmatrix}1 & 1 & 1\\2 & 2 & 2\\0 & 0 & 0\end{bmatrix}\begin{bmatrix}1 & 1 & 0\\1 & 2 & 2\\0 & 2 & 0\end{bmatrix}$$
$$\quad 0 \qquad\qquad 45° \qquad\qquad 90° \qquad\qquad 135°$$

$$\begin{bmatrix}1 & 2 & 0\\1 & 2 & 0\\1 & 2 & 0\end{bmatrix}\begin{bmatrix}0 & 2 & 0\\1 & 2 & 2\\1 & 1 & 0\end{bmatrix}\begin{bmatrix}0 & 0 & 0\\2 & 2 & 2\\1 & 1 & 1\end{bmatrix}\begin{bmatrix}0 & 2 & 0\\2 & 2 & 1\\0 & 1 & 1\end{bmatrix}$$
$$\qquad 180° \qquad 225° \quad 270° \qquad 315°$$
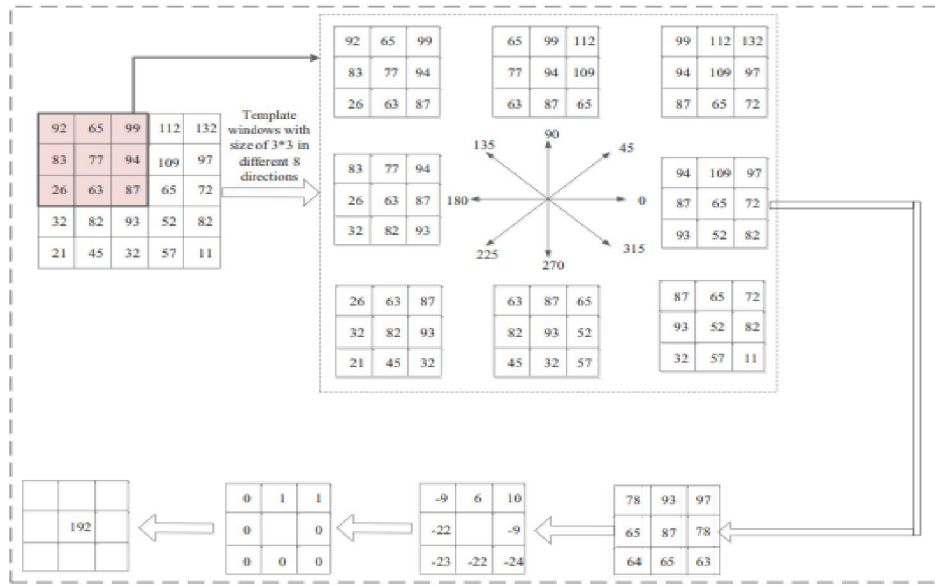
Fig. 7. Kirsch operator in eight directions.

Fig. 8. The calculation procedure of an actual NWALBP code example.

$$G_H(x,y) = I(x+1,y) - I(x-1,y) \quad (5)$$

$$G_V(x,y) = I(x,y+1) - I(x,y-1) \quad (6)$$

$$d(x,y) = arctan\left(\frac{G_H(x,y)}{G_V(x,y)}\right) \quad (7)$$

$$a = (x,y)\sqrt{\left(G_H(x,y)\right)^2 + \left(G_V(x,y)\right)^2} \quad (8)$$

The HOG operator is a description operator used to reflect the local gradient direction and gradient strength for a face image. The idea of HOG is utilising the gradient or edge direction distribution to reflect the edge or shape features for a target image. There are several merits as follows: (1) it is an efficient method for image edge acquisition which is particularly sensitive to image edge's shape information and gradient direction; (2) by dividing image into cells and doing local calculations, it is relatively easy to represent the relationship among local image pixels as well as match features in the process of image recognition; (3) it has good optical invariance as well as geometric invariance since HOG features are extracted based on small cells.

III. PROPOSED METHOD

3.1 Neighbourhood Weighted Average Local Binary Pattern (NWALBP)

Although there are several drawbacks, LBP and its extended operators still have a strong local description ability to image texture details for face recognition, and experts and scholars continue to improve them based on various fusion methods. Multi-texture CS-LBP [69] is proposed, which expands the LBP template window from the original size of 3 * 3 to modified size of 9 * 9, then makes local average based on blocks to effectively solve the problem that single pixel is vulnerable to illumination variations. However, there are still two problems: (1) multi-texture CS-LBP adopts a larger size of template window and it is likely to lead to insufficient description to image texture details. Moreover, it has been proved that using the template window with a size of 5*5 can acquire better description ability than with other sizes [70]. (2) Multi-texture CS-LBP does not fully consider that the stimulus intensities are different from the distances between different neighbourhood pixels and the center pixel [68]. In fact, the weight coefficients for different neighbourhood pixels should be adjusted according to those different distances when calculating the corresponding operator code.

To overcome the above-mentioned problems, an improved LBP operator called NWALBP is first proposed. For fully considering the strong correlations between pixel pairs in the neighbourhood, the template window with radius 1 and size of $3 * 3$ is extended to that with radius 2 and size of $5 * 5$. Then, the weighted average values of the neighbourhood pixels from the inner and outer layers adjacent to the centre pixel are calculated. The calculating procedures of NWALBP are very similar to that of LBP except for the different selected neighbourhood pixels adjacent to the central pixel. Figure 6 shows the inner and outer layer neighbourhood pixels in different directions of NALBP template window.

As shown in Figure 6, there is a template window with a size of 5*5, where x_c represents its centre pixel. $x_1, x_2, \ldots, x_8$ marked by green colour respectively represent the inner layer neighbourhood pixels that adjacent to the centre pixel x_c. $y_1, y_2 \ldots y_{16}$ marked by red colour respectively represent the outer layer neighbourhood pixels that adjacent to the centre pixel x_c. There are eight different neighbourhood regions circled by red wireframes for the template window, and each region is located in one template direction. Moreover, different weight of the inner layer and outer layer neighbourhood pixels are further decided by Kirsch operator with size of 3*3 for different neighbourhood regions, which replace the average weight for the single-layer neighbourhood pixels of the original LBP.

Based on the analysis of synergistic centre-surround receptive field model [68], it can be concluded that the center pixel's stimulus can be affected not only by the inner layer neighbourhood pixel but also by the outer layer neighbourhood pixel, and the effect is weakened with increase of the distance between the centre pixel and its surrounding pixels. Therefore, the weight values are set variously according to the different distances between the centre pixel and its neighbourhood pixels. Face recognition rate will be better if setting the weight ratio of the inner layer neighbourhood pixels and outer layer neighbourhood pixels as 2 [68]. Kirsch operator in eight directions of 0, 45, 90, 135, 180, 225, 270, 315 degrees are defined in Figure 7.

Suppose $w_i (\forall i = 0, 1, 2 \ldots P, P = 8)$ represents the ith weight calculated by the inner layer and outer layer neighbourhood pixels' grey values in the ith direction of template window. There are total eight directions in the template of window, and the corresponding weight values are given in the following equations:

$$w_0 = \frac{1}{9} \times \begin{pmatrix} 0 & 2 & 1 \\ 0 & 2 & 1 \\ 0 & 2 & 1 \end{pmatrix} \times \begin{pmatrix} x_2 & x_3 & y_6 \\ x_c & x_4 & y_7 \\ x_6 & x_5 & y_8 \end{pmatrix}$$

$$= \frac{1}{9} \times \left(2(x_3 + x_4 + x_5) + (y_6 + y_7 + y_8) \right) \quad (9)$$

$$w_1 = \frac{1}{9} \times \begin{pmatrix} 0 & 1 & 1 \\ 2 & 2 & 1 \\ 0 & 2 & 0 \end{pmatrix} \times \begin{pmatrix} y_3 & y_4 & y_5 \\ x_2 & x_3 & y_6 \\ x_c & x_4 & y_7 \end{pmatrix}$$

$$= \frac{1}{9} \times \left(2(x_2 + x_3 + x_4) + (y_4 + y_5 + y_6) \right) \quad (10)$$

$$w_2 = \frac{1}{9} \times \begin{pmatrix} 1 & 1 & 1 \\ 2 & 2 & 2 \\ 0 & 0 & 0 \end{pmatrix} \times \begin{pmatrix} y_2 & y_3 & y_4 \\ x_1 & x_2 & y_3 \\ x_8 & x_c & x_4 \end{pmatrix}$$

$$= \frac{1}{9} \times \left(2(x_1 + x_2 + x_3) + (y_2 + y_3 + y_4) \right) \quad (11)$$

$$w_3 = \frac{1}{9} \times \begin{pmatrix} 1 & 1 & 0 \\ 1 & 2 & 2 \\ 0 & 2 & 0 \end{pmatrix} \times \begin{pmatrix} y_1 & y_2 & y_3 \\ y_{16} & x_1 & x_2 \\ x_8 & x_8 & x_c \end{pmatrix}$$

$$= \frac{1}{9} \times \left(2(x_1 + x_2 + x_8) + (y_1 + y_2 + y_{16}) \right) \quad (12)$$

$$w_4 = \frac{1}{9} \times \begin{pmatrix} 1 & 2 & 0 \\ 1 & 2 & 0 \\ 1 & 2 & 0 \end{pmatrix} \times \begin{pmatrix} y_{16} & x_1 & x_2 \\ y_{15} & x_8 & x_c \\ y_{14} & x_7 & x_6 \end{pmatrix}$$

$$= \frac{1}{9} \times \left(2(x_1 + x_7 + x_8) + (y_{14} + y_{15} + y_{16}) \right) \qquad (13)$$

$$w_5 = \frac{1}{9} \times \begin{pmatrix} 0 & 2 & 0 \\ 1 & 2 & 2 \\ 1 & 1 & 0 \end{pmatrix} \times \begin{pmatrix} y_{15} & x_8 & x_c \\ y_{14} & x_7 & x_6 \\ y_{13} & y_{12} & y_{11} \end{pmatrix}$$

$$= \frac{1}{9} \times \left(2(x_6 + x_7 + x_8) + (y_{12} + y_{13} + y_{14}) \right) \qquad (14)$$

$$w_6 = \frac{1}{9} \times \begin{pmatrix} 0 & 0 & 0 \\ 2 & 2 & 2 \\ 1 & 1 & 1 \end{pmatrix} \times \begin{pmatrix} x_8 & x_c & x_4 \\ x_7 & x_6 & x_5 \\ y_{12} & y_{11} & y_{10} \end{pmatrix}$$

$$= \frac{1}{9} \times \left(2(x_5 + x_6 + x_7) + (y_{10} + y_{11} + y_{12}) \right) \qquad (15)$$

$$w_7 = \frac{1}{9} \times \begin{pmatrix} 0 & 2 & 0 \\ 2 & 2 & 1 \\ 0 & 1 & 1 \end{pmatrix} \times \begin{pmatrix} x_c & x_4 & y_7 \\ x_6 & x_5 & y_8 \\ y_{11} & y_{10} & y_9 \end{pmatrix}$$

$$= \frac{1}{9} \times \left(2(x_4 + x_5 + x_6) + (y_8 + y_9 + y_{10}) \right) \qquad (16)$$

Furthermore, the NWALBP code can be defined in Equations (17) and (18):

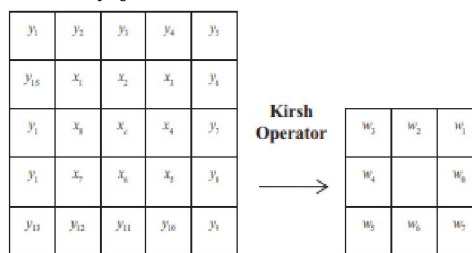$$NWALBP = \sum_{i=0}^{P-1} s(w_i - x_c) \, 2^i, P = 8 \qquad (17)$$

Fig. 9. Weight values in eight different directions calculated by Kirsch operator.

$$s(x) = \begin{cases} 1, & if \ x \geq 0 \\ 0, & if \ x < 0 \end{cases} \qquad (18)$$

The calculation procedure of an actual NWALBP code example is depicted in Figure 8.

3.2 Center Symmetric NWALBP (CS-NWALBP)

Inspired by CS-LBP, CS-NWALBP is further proposed based on modifying the NWALBP. w0, w1, w2, w3, w4, w5, w6, w7 are calculated by Equations (9)–(16) and illustrated in Figure 9. Our proposed CS-NWALBP code can be expressed in Equations (19) and (20):

$$CS - NWALBP \sum_{i=0}^{P-1} s\left(w_i - w_{i+(P/2)}\right)2^i, P = 8 \qquad (19)$$

$$s(x) = \begin{cases} 1, & if \ w_i - w_{i+(P/2)} \geq t \\ 0, & if \ w_i - w_{i+(P/2)} < t \end{cases} \qquad (20)$$

Where w_i and $w_{i+(P/2)}$ are the weight values of center symmetric pixel pairs. The calculation procedure of an actual CSNWALBP code example is depicted in Figure 10. It can be easily seen that the NWALBP operator can extract a total of 28 (256)-dimensional histogram features, while the CS-
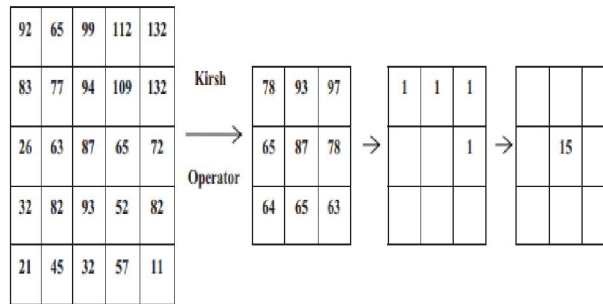

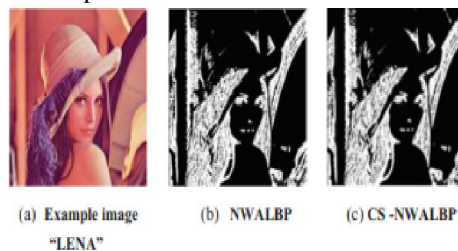Fig. 10. The calculation procedure of an actual CS-NWALBP code example.

Fig. 11. Example image 'LENA' and its corresponding NWALBP and CS-NWALBP feature images.

NWALBP operator only extracts a total of 24 (16)-dimensional histogram features. Therefore, compared with NWALBP, the CS-NWALBP operator can reduce computation load, as well as feature extraction dimensions. The classical image 'LENA' and its corresponding NWALBP and CS-NWALBP feature extraction images are given in Figure 11.

3.3 Feature fusion of CS-NWALBP and HOG (CS-NWALBP+HOG)

LBP has the characteristics of greyscale and rotation invariance, as well as the strong description ability to image texture details. HOG is also robust to edge information, gradient direction information, and illumination variations. By taking full advantages of LBP and HOG, an improved image recognition algorithm based on feature fusion of CSNWLBP and HOG is proposed, called CS-NWALBP+HOG.

The feature extraction process of CS-NWALBP+HOG is shown in Figure 12 and depicted in the following:

Step I: Dividing the extracted feature images into a series of blocks uniformly;

Step II: Utilising the CS-NWALBP operator to extract local feature images for each block image; and obtaining the statistics of image blocks using histograms;

Step III: Constructing the CS-NWALBP histograms for the whole image by concatenating the statistical histograms of each block in sequence;

Step IV: Constructing the final fusion features by concatenating the CS-NWALBP histogram features;

Step V: Matching and accomplishing face recognize by the k-nearest neighbour (KNN) classifier based on Chisquare distance.
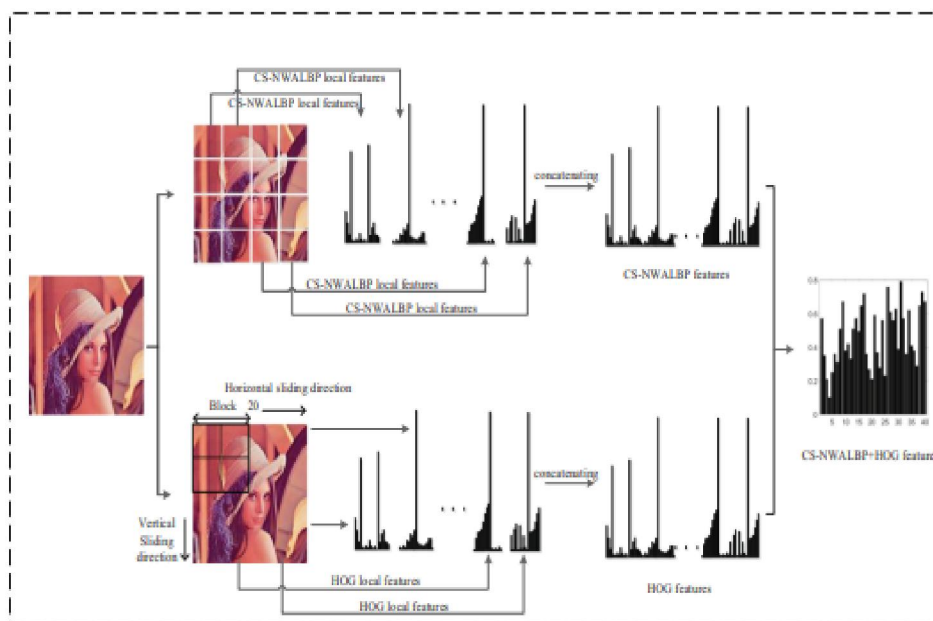
Impact Factor: 6.252

Fig.12. Feature extraction process of CS-NWALBP+HOG.

TABLE I: Experimental Environment Settings.

Index	Environment	Configuration
1	Operating system	Window 7 64 bit
2	CPU	17,2.93 GHz
3	Memory	4.0 G
4	Hard disk	500 G
5	Program Design	Matlab 2015b

IV. EXPERIMENTS AND ANALYSIS

To verify the effectiveness of our proposed method, several experiments are conducted on different public databases, which have been widely used in the field of face recognition, such as CMUPIE, Yale B, and FERET etc. The experimental environment settings are listed in Table I.

4.1 CMUPIE Database

LBP proposed by CMUPIE database contains 41,368 face images captured from 68 individuals, each of which has different expressions, poses and illumination conditions. Partial face images of CMUPIE are shown in Figure 13.

Fig. 13. Partial face images of CMUPIE.

4.2 Effects of Different Block Sizes on Recognition Rate

Face images of 40 individuals with more serious influence of illumination are selected from CMPUIE to construct the experiment set. The first half of these selected images are used as the training samples, and the rest images are used as the experimental test images. To ensure the accuracy of experimental results, we repeat one experiment 20 times and make average of the results. Experiment results are illustrated in Figure 14, which give the effects of different block sizes on recognition rate of CS-NWALBP, CS-LBP, as well as our proposed CSNWALBP+HOG.

As shown in Figure 14, the recognition rate on CMUPIE database increases with the increase of the block size at first, and achieves the maximum value with a size of 12*12, then decreases with the increase of the block size. From the

trend analysis of the above curve, if with smaller block sizes, the extracted features are over localized and has too little histogram information; on the contrary, if with larger block sizes, the extracted features are insufficient and unable to describe the local texture information. Therefore, it is very important to choose the suitable block sizes for face recognition.
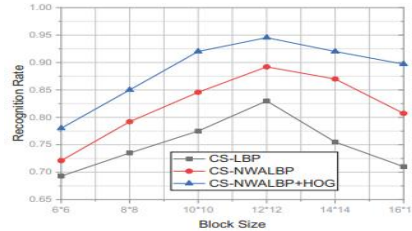

Fig. 14. Effects of different block sizes on recognition rate.

TABLE 2: Recognition Rate Comparisons On Database Cumpie.

Algorithm	Training	sampling	numbers		
	2	4	8	16	32
CS-LBP[48]	0.600	0.628	0.678	0.720	0.828
LTP[71]	0.613	0.628	0.694	0.735	0.828
LBP[48]	0.600	0.633	0.679	0.720	0.820
LGS[64]	0.623	0.661	0.664	0.750	0.833
SLGS[65]	0.655	0.694	0.729	0.820	0.867
WLD[50]	0.682	0.722	0.786	0.870	0.900
L-PDE[72]	0.654	0.756	0.828	0.902	0.913
WLBP[62]	0.567	0.712	0.812	0.859	0.936
NWALBP	0.698	0.710	0.732	0.840	0.880
CS-NWALBP	0.663	0.725	0.756	0.850	0.900
CS-NWALBP+HOG	0.728	0.761	0.798	0.882	0.942

4.3 Recognition Rate Comparisons

Under the optimal condition with a block size of 12*12 (as discussed in Section 4.1.1), several experiments on recognition rate comparisons are conducted to verify the effectiveness of our proposed CS-NWALBP+ HOG, and the corresponding results are listed in Table II.

From Table II, it can be observed that the recognition rate of algorithms increases with the increase in the number of training samples. When the number of samples is small, including our proposed algorithm, the final recognition rates of all algorithms are relatively low. Table I shows that NWALBP can improve the recognition rate by 6% if compared with LBP, which indicates that the neighbourhood structure with a size of 5*5 can better reflect grey level image variations, as well as make the weighted average for neighbourhood pixels effectively overcome noise [68]. The experimental comparisons show that the highest recognition rate of features extracted by the proposed CS-NWALBP+HOG algorithm under complex illuminations can achieve 94.2%, which is about 2.9% higher than that of LPDE. Therefore, CS-NWALBP+HOG is more robust to illumination variations. In the case of training number 8 and 16, the L-PDE method [72] achieves better results than the proposed method. However, the proposed method obtains the best performance when the training number is 32. It is shown that the proposed method relies on more training samples and it needs to be further promoted in the future work.

Furthermore, we also compare some methods based on deep learning. As shown in Table III, Moreover, the deep learning methods including VGGNet, ResNet and some improved methods achieve relevant lower recognition rate because of the small sample.

TABLE III: The Comparison Of Recognition Rate In Cumpie.

Methods	Recognition rate%
VGGNet[73]	93.2
ResNet[74]	90.4

LBP+CNN[75]	94.1
CS-NWALBP+HOG	94.2

TABLE IIV: Recognition Time Comparisons.

Algorithm	Recognition time (ms)
LBP[48]	22.36
LTP[71]	24.87
LGS[64]	24.22
SLGS[65]	26.77
WLD[50]	25.31
WLBP[62]	53.34
HOG[49]	21.21
NWALBP	17.56
CS-NWALBP	11.91
CS-NWALBP+HOG	28.12

4.4 Recognition Time Comparisons

As can be seen from Table IV, compared with other face recognition algorithms, CS-NWALBP spends the least time on face recognition on CMUPIE database. Therefore, the experimental results show that CS-NWALBP not only takes less time than LBP, but also improves the recognition rate. It has been fully proved that CS-NWALBP is able to compare pairs of centre symmetric pixels, which can not only effectively reduce the amount of computation but also avoid the mutation of centre symmetric pixels due to the influence of noise, enhance image's anti-noise capability and improve the recognition rate. Although our proposed CS-NWALBP+HOG indeed increases the time spent on face recognition to some extent, if compared with WLBP, the consuming time is still less, and the recognition rate is improved significantly, which fully demonstrates the effectiveness of CS-NWALBP+HOG.

Fig. 15. Partial face images of FERET.

4.5 FERET Database

As a larger public face image database, FERET contains 14,501 face images captured from 1199 individuals, with different expressions, poses and illumination variations, including five subsets: fa, fb, fc, dup I and dup II. Partial face images of FERET are shown in Figure 15.

Face images of 40 individuals with more serious influence of illumination and posture variations are selected from FERET to construct the experiment set. Each individual corresponds to 10 images, and each image is with a size of 80*80. For each individual, six of any face images are taken as the training images and the remaining four images as the test images. Under different block sizes, performances of NWALBP, CS-NWALBP and CSNWALBP+HOG are compared to find the best block size. To make the results reliable, each group of experiments is carried out 10 times respectively, and the average value is taken as the final result.

Next, individuals of FERET database are randomly selected. The 1st, 3rd, 5th and 7th images from each of the selected individuals are further used to form the training set, and the remaining images form the test set. From the trend analysis of the curve shown in Figure 16, the recognition rate on FERET database can achieve the maximum value if the block size is set properly as 10*10. Therefore, under the optimal condition with a block size of 10*10, several experiments on recognition rate comparisons are conducted to verify the effectiveness of our proposed algorithms.

The comparison results from Table V show that our proposed algorithms are more robust to illumination noise if compared with other algorithms. The recognition rate of CSNWALBP+HOG is 96.66% when the number of training samples is 7, which has obviously better performance.

4.6 Yale B Database

Yale B database contains 640 face images captured from 10 individuals with nine different poses and illumination conditions. Partial face images of Yale B are shown in Figure 17.
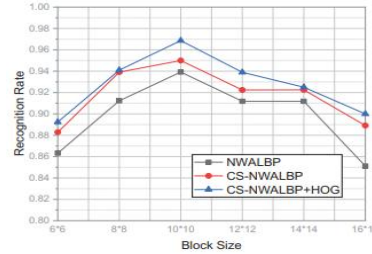

Fig. 16. Effects of different block sizes on recognition rate.

TABLE V: Recognition Rate Comparisons On Database FERET.

	Training	sampling	numbers	
Algorithm	**1**	**3**	**5**	**7**
LBP[48]	0.652	0.703	0.790	0.844
LTP[71]	0.659	0.680	0.683	0.830
LGS[64]	0.667	0.679	0.639	0.722
SLGS[65]	0.700	0.722	0.733	0.758
WLD[50]	0.722	0.714	0.750	0.833
WLBP[62]	0.667	0.786	0.806	0.850
WLDs[63]	0.723	0.755	0.898	0.880
NWALBP	0.716	0.818	0.835	0.912
CS-NWALBP	0.750	0.837	0.860	0.928
CS-NWALBP+HOG	0.791	0.850	0.895	0.966

Yale B database is divided into five subsets according to the direction of illumination relative to the camera axis, namely, S1, S2, S3, S4 and S5. Among these subsets, those images in the subsets S4 and S5 were obtained under very poor illumination conditions, and therefore are selected to test the relationship between recognition rates and block sizes for different algorithms. In S4 and S5, the first two-thirds of images from each of the individuals are selected as the training set, and the rest images are set as the test set. To ensure the accuracy of experimental results, each group of experiments is done 10 times, and the average value is taken as the final recognition rate.

As shown in Figure 18, under the optimal condition with a block size of 12*12, our proposed NWALBP, CS-NWALBP and CS-NWALBP+HOG can obtain relatively high recognition rate. Thus, several experiments on recognition rate comparisons are conducted with a block size of 12*12. In each subset of Yale B database, two-thirds of images selected from each of individual are selected as the training set, and the rest images are verified as the test set. Each group of experiments is done 10 times, and the average value is taken as the final recognition rate. In Figure 18, the histograms of recognition rate for different algorithms are marked by S1, S2, S3, S4 and S5, respectively, corresponding to the performance results on five subsets. S6 represents the final average recognition rate calculated based on five existing subsets.

As illustrated in Figure 19, our proposed CS-NWALBP+ HOG shows superior performance on different subsets, especially on three subsets of S3, S4 and S5 with poorer illumination conditions. In the meanwhile, on five subsets with different illumination conditions, our proposed algorithms always maintain higher recognition rates, which fully show that their performance is not easily affected by illumination noise and has better stability. On the subset of S6, the average recognition rate of CS-NWALBP+HOG is higher than CS-NWALBP, indicating the effectiveness of feature fusion method.
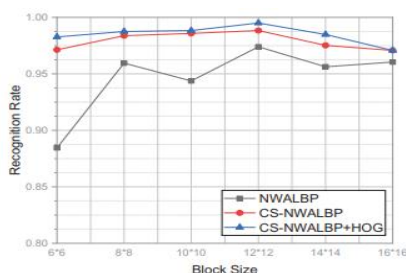

Fig. 17. Partial face images of Yale B.

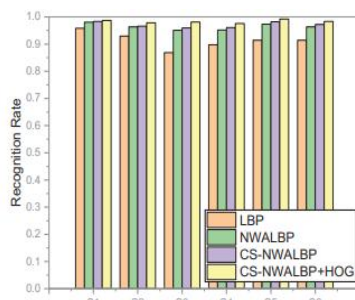Fig. 18. Effects of different block sizes on recognition rate.

Fig. 19. Recognition rate on different Yale B subsets.

V. CONCLUSION

In this paper, we propose a face recognition attendance system method CSNWALBP and a fusion algorithm CS-NWALBP+HOG based on LBP and HOG to overcome the problems of LBP, HOG and their related improved operators. A series of simulation experiments on the commonly used CMUPIE, FERET and Yale B databases are conducted and verify the effectiveness of our methods. In the future, for improving the recognition rate, it still needs to further study how to configure the adaptive weight coefficients. Moreover, the future research work should also include how to reduce the recognition time of the classifier and in the meanwhile improve the corresponding classification ability.

ACKNOWLEDGMENT

REFERENCES

[1]. Li, S.Z., Jain, A.K.: Handbook of Face Recognition (2nd ed.). Springer, New York (2011).

[2]. Jain, A.K., et al.: Face recognition: Some challenges in forensics. IEEE International Conference on Automatic Face & Gesture Recognition. IEEE Computer Society (2011).

[3]. Nolazco-Flores, J.A., et al.: Addressing the illumination challenge in two dimensional face recognition: A survey. IET Comput. Vision 9(6), 978– 992 (2015).

[4]. Han, H., et al.: A comparative study on illumination pre-processing in face recognition. Pattern Recognition. 46(6), 1691–1699 (2013).

[5]. Beyerer, J., et al.: Pre-processing and image enhancement. In: Machine Vision. Springer, Berlin/Heidelberg (2016).

[6]. Li, M.: Research and implementation on enhancement technology for low illumination image. Nanjing University of Posts and Telecommunications (2016).

[7]. Kim, Y.T.: Contrast enhancement using brightness preserving histogram equalization. IEEE Trans. Consum. Electron. 43(1), 1–8 (1997).

[8]. Wang, Y., et al.: Image enhancement based on equal area dualistic sub image histogram equalization method. IEEE Trans. Consum. Electron. 45(1), 66–75 (1999).

[9]. Chen, S.D., Ramli, and A.R.: Minimum mean brightness error Bi-histogram equalization in contrast enhancement. IEEE Trans. Consum. Electron. 49(4), 1310–1319 (2003).

[10]. Reza, A.M.: Realization of the contrast limited adaptive histogram equalization (CLAHE) for real-time image enhancement. J. VLSI Sig. Proc. 38(1), 35–44 (2004).

[11]. Sheet, D., et al.: Brightness preserving dynamic Fuzzy histogram equalization. IEEE Trans. Consum. Electron. 56(4), 2475–2480 (2010).

[12]. Kim, W.: Contrast enhancement using histogram equalization based on logarithmic mapping. Opt. Eng. 51(6), 067002 (2012).

[13]. Fries, R.W., Modestino, J.W.: Image enhancement by stochastic homomorphic filtering. IEEE Trans. Acoust. Speech Signal Process. 27(6), 625–637 (1980).

[14]. Zhang, X.M., Shen, and L.S.: Image contrast enhancement by wavelet based homomorphic filtering. Chin J. Electron. 4, 100–102 (2001).

[15]. Fan, C.N., Zhang, and F.Y.: Homomorphic filtering based illumination normalization method for face recognition. Pattern Recognition. Letts. 32(10), 1468– 1479 (2011).

[16]. Xu, L., et al.: Suppression of the fluctuation effect in terahertz imaging using homomorphic filtering. Chin. Opt. Lett. 11(8), 081201 (2013).

[17]. Shahamat, H., Pouyan, and A.A.: Face recognition under large illumination variations using homomorphic filtering in spatial domain. J. Visual Commun. Image Represent. 25(5), 970–977 (2014).

[18]. Hassan, M.F.A., et al.: Enhancement of under-exposed image for object tracking algorithm through homomorphic filtering and mean histogram matching. Adv. Sci. Letters 23(11), 11257–11261 (2017).

[19]. Land, E.H.E.: Lightness and Retinex theory. J. Opt. Soc. Am. 61(1), 1–11 (1971).

[20]. Park, Y.K., Kim, J.K.: A new methodology of illumination estimation/normalization based on adaptive smoothing for robust face recognition. IEEE International Conference on Image Processing, 2007. ICIP 2007. IEEE, 149–152 (2007).

[21]. Jiang, Y.X., et al.: A method for image enhancement based on light compensation. Chin. J. Electron. 37(A04), 151–155 (2009)

[22]. Wang, G., et al.: Retinex theory based active contour model for segmentation of inhomogeneous images. Digital Signal Process. 50, 43–50 (2015).

[23]. Park, S., et al: Low-light image enhancement using Variational optimization-based Retinex model. IEEE Trans. Consum. Electron. 63(2), 178–184 (2017).

[24]. Jie Z., al.: Low-light image enhancement based on iterative multi-scale guided filter Retinex. J. Graphics 39(1), 1–11 (2018).

[25]. Zhang, T., et al.: Face recognition under varying illumination using gradient faces. IEEE Trans. Image Process. 18(11), 2599–2606 (2009).

[26]. Tzimiropoulos, G., et al.: Principal component analysis of image gradient orientations for face recognition. 2011 IEEE International Conference on Automatic Face & Gesture Recognition and Workshops (FG 2011). IEEE, 553–558 (2011).

[27]. Xu, X., et al.: Perception-based gradient domain enhancement of images. J. Comput.-Aided Des. Comput. Graphics 16(2), 130–135 (2011).

[28]. Tzimiropoulos, G., et al: Subspace learning from image gradient orientations. IEEE Trans. Pattern Anal. Mach. Intel. 34(12), 422–433 (2013).

[29]. Ma, P., et al.: Robust face recognition via gradient-based sparse representation. J. Electron. Imaging 22(1), 3018–3026 (2013).

[30]. Chen, B.Q., Liu, H.L.: Algorithm for foggy image enhancement based on the total Variational Retinex and gradient domain. J. Commun. 35(6), 139– 147 (2014).

[31]. Wold, S.: Principal component analysis. Chemo. Intel. Lab. Syst. 2(1), 37–52 (1987).

[32]. Kim, W., et al.: SVD face: Illumination-invariant face representation. IEEE Signal Process. Letts. 21(11), 1336–1340 (2014).

[33]. Kim, K.I., et al: Face recognition using kernel principal component analysis. IEEE Signal Process. Letts. 9(2), 40–42 (2002).

[34]. Gottumukkal, R., Asari, V.K.: An improved face recognition technique based on modular PCA approach. Pattern Recognition. Lett. 25(4), 429–436 (2004).

[35]. Yang, J., et al.: two-dimensional PCA: A new approach to appearance-based face representation and recognition. IEEE Trans. Pattern Anal. Mach. Intel. 26(1), 131–137 (2004).

[36]. Dandpat, S.K., Meher, S.: Performance improvement for face recognition using PCA and two-dimensional PCA. International Conference on Computer Communication & Informatics. IEEE (2013).

[37]. Tan, K., Chen, S.: Adaptively weighted sub-pattern PCA for face recognition. Neurocomputing 64(1), 505–511 (2005).

[38]. Zhang, Q., Li, B.X.: Discriminative K-SVD for dictionary learning in face recognition. 2010 IEEE Computer Society Conference on Computer Vision and Pattern Recognition. IEEE, (2010).

[39]. Belavadi, B., et al.: An investigation of SVD and ridge let transform for illumination and expression invariant face recognition. Adv. Intell. Syst. Comput. 320, 31–38 (2015).

[40]. Lee, M.S., et al.: Face recognition under variant illumination using PCA and wavelets. Scandinavian Conference on Image Analysis. Springer-Verlag (2009).

[41]. Wang, J.W., Chen, and T.H.: Face recognition based on adaptive singular value decomposition in the wavelet domain. International Conference on Human-Computer Interaction. 413–418 (2017).

[42]. Xide, W.U., Qingbiao, and Z.: Variable illumination face recognition based on correlation filter and 2DPCA. Comput. Eng. Appl. 6, 2655–2660 (2014).

[43]. James, E.A.K., Annadurai, S.: Implementation of incremental linear discriminant analysis using singular value decomposition for face recognition. First International Conference on Advanced Computing. IEEE, (2010).

[44]. Zhang, Y., et al: Face recognition under varying illumination based on singular value decomposition and retina modelling. Multimedia Tools Appl. 77, 28355–28374 (2018).

[45]. Zhang, G., et al.: Singular value decomposition based virtual representation for face recognition. Multimedia Tools Appl. 77(11), 1–16 (2017).

[46]. 46. Oh, J.H., Kwak, N.: Generalization of linear discriminant analysis using Lp-norm. Pattern Recognit. Lett. 34(6), 679–685 (2013).

[47]. Chen, W., et al.: Illumination compensation and normalization for robust face recognition using discrete cosine transform in logarithm domain. IEEE Trans. Cybern. 36(2), 458–466 (2006).

[48]. Ojala, T., et al.: A comparative study of texture measures with classification based on featured distributions. Pattern Recognit. 29(1), 51–59 (1996).

[49]. Dalal, N., Triggs, B.: Histograms of oriented gradients for human detection. 2005 IEEE Computer Society Conference on Computer Vision and Pattern Recognition (CVPR'05). IEEE, (2005).

[50]. Jie, C., et al.: WLD: A robust local image descriptor. IEEE Trans. Pattern Anal. Mach. Intell. 32(9), 1705–1720 (2010).

[51]. Ojala, T., et al.: Multiresolution gray-scale and rotation invariant texture classification with local binary patterns. IEEE Trans. Pattern Anal. Mach. Intell. 24(7), 971–987 (2002).

[52]. Heikkilä, M., et al.: Description of interest regions with local binary patterns. Pattern Recognit. 42(3), 425–436 (2009).

[53]. He, C., et al.: A Bayesian local binary pattern texture descriptor. 19th International Conference on Pattern Recognition (ICPR 2008), December 8– 11, 2008, Tampa, Florida, USA. IEEE, (2008).

[54]. Guo, Z., et al.: A completed modelling of local binary pattern operator for texture classification. IEEE Trans. Image Process. 19(6), 1657–1663 (2010).

[55]. Zhang, J.Y., et al.: Face recognition based on weighted local binary pattern with adaptive threshold. J. Electron. Inf. Technol. 36(6), 1327–1333 (2014).

[56]. Cai, Z.B., Gu, Z.H.: A real-time visual object tracking system based on Kalman filter and MB-LBP feature matching. Multimedia Tools Appl. 75(4), 2393–2409 (2016).

[57]. Déniz, O., et al.: Face recognition using histograms of oriented gradients. Pattern Recognit. Lett. 32(12), 1598–1603 (2011).

[58]. Guo, J.X., Chen, W.: Face recognition based on HOG multi-feature fusion and random forest. Comput. Sci. 40(10), 279–283 (2013).

[59]. Sun, Y., Liu, and G.Q.: Face recognition method based on HOG and LBP feature. Comput. Eng. 41(9), 205–208 (2015).

[60]. Wan, Y., et al.: Research on fusion of layered CS-LBP and HOG for face recognition. J. Wuhan Univ. Technol. (Transp. Sci. Eng.) 38(4), 801–805 (2014).

[61]. Packer, O.S., Dacey, D.M.: Synergistic center-surround receptive field model of monkey H1 horizontal cells. J. Vision 5(11), 1038–1054 (2005).

[62]. Liu, F, et al.: WLBP: Weber local binary pattern for local image description. Neurocomputing 120, 325–335 (2013).

[63]. Li, S., et al.: Face recognition using Weber local descriptors. Neurocomputing 122, 272–283 (2013).

[64]. Abusham, E.: Face verification using local graph stucture (LGS). International Symposium on Biometrics and Security Technologies. IEEE, 79–83 (2014).

[65]. Abdullah, M.F.A., et al.: Face recognition with symmetric local graph structure (SLGS). Expert Syst. Appl. 41(14), 6131–6137 (2014).

[66]. Gao, T., et al.: Image feature representation with orthogonal symmetric local weber graph structure. Neurocomputing 240(31), 70–83 (2017).

[67]. Gao, T., et al.: Local difference ternary sequences descriptor based on unsupervised min redundancy mutual information feature selection. Multidimensional Syst. Signal Process. (2020), https://doi.org/10.1007/s11045-018-0595-z.

[68]. Gao, T., et al.: Illumination-insensitive image representation via synergistic weighted center-surround receptive field model and weber law. Pattern Recognit. 69, 124–140 (2017).

[69]. Cui, K., et al.: Multi-view face detection algorithm based on multi-texture CS-LBP Features. J. Jilin Univ. (Sci. Ed.) 56, (03), 148–154 (2018).

[70]. Ren, J., et al.: Optimizing LBP structure for visual recognition using binary quadratic programming. IEEE Signal Process Lett. 21(11), 1346–1350 (2014).

[71]. Tan, X., Triggs, B.: Enhanced local texture feature sets for face recognition under difficult lighting conditions. IEE. Image Process. 19(6), 1635–1650 (2010).

[72]. Fang, C., et al.: Feature learning via partial differential equation with applications to face recognition. Pattern Recognit. 69(3), 14–25 (2017).

[73]. Parkhi, O.M., et al.: Deep face recognition. British Machine Vision Conference, (2015).

[74]. Wen, Y., et al.: A discriminative feature learning approach for deep face recognition. European Conference on Computer Vision. Cham: Springer, 499–515 (2016).

[75]. Ke, P., et al.: A novel face recognition algorithm based on the combination of LBP and CNN. 2018 14th IEEE International Conference on Signal Processing (ICSP). IEEE, 539–543 (2018).

[76]. Wang, Q., et al.: Pixel-wise crowd understanding via synthetic data. Int. J. Comput. Vision 129(1), 225–245 (2021).

[77]. Wang, Q., et al.: Detecting coherent groups in crowd scenes by multitier clustering. IEEE Trans. Pattern Anal. Mach. Intell. 42(1), 46–58 (2018).

[78]. Wang, Q, et al.: NWPU-Crowd: A large-scale benchmark for crowd counting and localization IEEE Trans. Pattern Anal. Machine Intell. (2020), https://doi.org/10.1109/TPAMI.2020.3013269.

BIOGRAPHY

Vrunda Mahajan, MTech (pursing) at department of computer science and engineering, SSGBCOET, Bhusawal. Interested in fields of computer vision and image understanding, pattern recognition, image processing, big data.

Dr. Priti Subramanium, Assistant Professor, M.E. (Digital Electronics), Ph.D. at department of computer science and engineering, SSGBCOET, Bhusawal. Research interest in wireless communication with the experience of 19 years.